EUROPEAN ORGANIZATION FOR NUCLEAR RESEARCH

European Laboratory for Particle Physics

CERN - SL DIVISION

CERN-SL-97-67 (BI)

Comparison of Different Methods for Transverse Emittance Measurement and Recent Results from LEP

Claude Bovet, Claude Fischer and Roland Jung

Abstract

The knowledge of its position and angular transverse distributions is of utmost interest to assess the good behaviour of a beam within an accelerator. After a short reminder of beam "emittance" definitions, a review is made of various measurement techniques used so far both in single pass machines and colliders. Results of measurements made at CERN in the future LHC injection complex and in LEP are presented and discussed.

Paper presented at the Third European Workshop on Beam Diagnostics and Instrumentation for Particle Accelerators (DIPAC 97), Frascati, Italy, 12-14 October 1997

Geneva, Switzerland
December, 1997

Comparison of Different Methods for Transverse Emittance Measurement and Recent Results from LEP

Claude Bovet, Claude Fischer and Roland Jung
CERN, Geneva, Switzerland

Abstract

The knowledge of its position and angular transverse distributions is of utmost interest to assess the good behaviour of a beam within an accelerator. After a short reminder of beam "emittance" definitions, a review is made of various measurement techniques used so far both in single pass machines and colliders. Results of measurements made at CERN in the future LHC injection complex and in LEP are presented and discussed.

1 INTRODUCTION

Some words are needed on the definition of transverse emittance which is a hyper volume

$$E = \iint dq_x dp_x \iint dq_y dp_y$$

containing the co-ordinates of transverse positions q_x, q_y and transverse momenta p_x, p_y of most particles belonging to the beam. When the motion is energy conservative the phase space of the beam can change shape but its volume remains constant through Liouville's theorem. In paraxial optics the canonical co-ordinates are replaced by x, x', y, y', where the derivatives are with respect to the longitudinal co-ordinate and the space is, more precisely, called *trace space*. When the external forces are periodic, linear and without x-y coupling the trace space volume is a hyper-ellipsoid described by Courant&Snyder's invariants in the trace planes x,x' and y, y':

$$\gamma x^2 + 2\alpha x x' + \beta x'^2 = \text{const.}$$

This invariant has the shape of an ellipse in the x, x' trace plane and represents the various possible positions of a particle. All particles belong to similar ellipses with a surface proportional to the particle's transverse energy. Therefore the most significant emittance definition is:

$$<\varepsilon>^2 = <x^2><x'^2> - <x\,x'>^2 \ ,$$

which corresponds to the area divided by • of the ellipse traced by a particle with average transverse beam energy.

At low energy, when space charge plays an important role, the beam envelope can be described by the equations:

$$X'' + k_x X - \frac{2K}{X+Y} - \frac{\varepsilon_x^2}{X^3} = 0$$

$$Y'' + k_y Y - \frac{2K}{X+Y} - \frac{\varepsilon_y^2}{Y^3} = 0$$

which have a self consistent solution for the Kapshinsky-Vladimirsky (K-V) uniform distribution inside the 4-D ellipsoid. These equations are also satisfied for the beam rms sizes [1] and the relationship between emittances is:

$$\varepsilon_{x,y} = 4 < \varepsilon_{x,y} >$$

At high energy and for all electron storage rings, transverse distributions tend to become Gaussian with a profile distribution of the type:

$$P(x) = \frac{1}{\sqrt{2\pi}\,\sigma_x} \quad e^{-\frac{x^2}{2\sigma_x^2}}$$

and a trace plane betatron amplitude distribution:

$$P(a) = \frac{a}{\sigma_x} \quad e^{-\frac{a^2}{2\sigma_x^2}}$$

where $\sigma_a = \bullet 2\ \sigma_x$.

For emittance determination, most techniques measure profiles P(x) or P(x') projected onto the x or x' axis and some measure the betatron amplitude distribution P(a). Table 1 summarises some emittance definitions.

The rms emittance has always been used in electron machines and is now more and more common in the discussion of high energy hadron colliders because it is so strongly linked to luminosity. It contains only a small fraction of the beam but it is well understood that the aperture of the machine must be at least 6 to 10 sigma's.

Table 1. Characteristics of some emittance definitions

Application	Emittance	Betatronic amplitude in terms of σ_x or σ_a		•P(x)dx (profile)	•P(a)da (ellipse)
rms beam size	<ε>	σ_x	$0.71\ \sigma_a$	64 %	39 %

K-V distribution Lapostolle (CERN)	$\varepsilon = 4\langle\varepsilon\rangle$	$2\,\sigma_x$	$1.41\,\sigma_a$	95 %	86 %
FermiLab option	$\varepsilon = 6\langle\varepsilon\rangle$	$2.45\,\sigma_x$	$1.73\,\sigma_a$	98.5 %	95 %

2 EMITTANCE MEASUREMENT TECHNIQUES

Pepper-pot

A pepper-pot is a sieve which separates the beam into several beamlets whose divergence in both transverse directions can be observed beyond a small drift length (see Fig. 1). In the early days the detector was a photographic plate which could be analysed after development, with a densitometer.

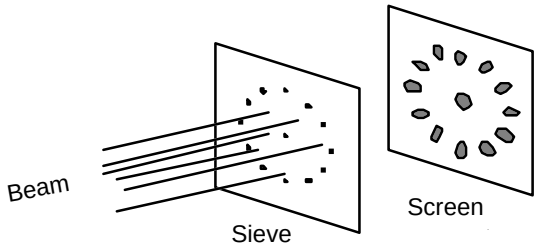

Fig. 1. Schematics of the pepper-pot.

Nowadays this method is still used to optimise the brightness of an electron gun, measuring emittances in the range 5 to 200 • μm rad [2]. The sieve can be made of a titanium sheet 20 μm thick, where holes of 30 μm diameter are machined. A thin scintillator film is used to visualise the electron density pattern which is observed with an optical microscope able to focus the image onto a MCP in front of a CCD camera. With a few 10^5 pixels, even a complex multiple image can be scanned to restore the 4-D trace space density.

In another variant of this technique the holes are replaced by a series of slits and such a grid can be used to analyse a 2-D trace plane.

Dynamic emittance scan

Another possibility consists of using a single slit on which the beam is swept in the perpendicular direction. The divergent beam that goes through the slit is then rotated by 90^o in the trace plane and reaches the wire array of a secondary emission (SEM) grid detector (see Fig. 2).

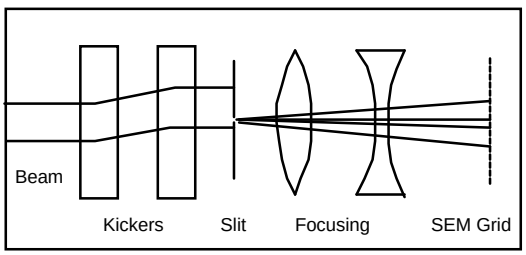

Fig. 2. Schematics of dynamic emittance scan

Such a system exists in the transfer line from Linac2 to CPB at CERN [3] and allows to take the data necessary for a full 2-D analysis, during the passage of a unique linac pulse. A total of 96 samples of each wire are taken during a sweep of 12 μs requiring 24 ADCs at a sampling frequency of 8 MHz. Both transverse dimensions, as well as the longitudinal one, can be analysed in succession.

Three gradients

This method serves to measure the beam emittance, say, at the end of a transfer channel, with the help of three different projections of the trace plane density. The detector is generally destructive because the beam cannot be recuperated after it has been strongly focused or defocused. There are various mathematical ways to uncover the emittance shape and size. One of the more convincing ones uses many measurements in order to fit a theoretical curve from which the Twiss parameters can be deduced [4].

Three profile monitors

A more practical method used in transfer lines consists of measuring profiles at three successive locations with thin monitors like SEM grids, SEM wires or screens. These monitors are semi-destructive and are moved into the beam at measurement time. Their resolution must be better than one sigma of the profile to be analysed. Figure 3 shows the ideal case where the three monitors are separated by drift spaces [5].

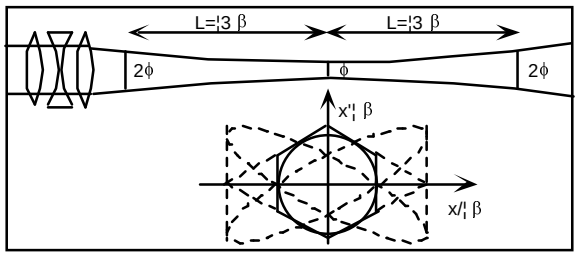

Fig. 3. Three monitors separated by drift spaces.

In the more general case the detectors are placed in a FODO array with about 60^o phase advance between them. The dispersion function is well known in a transfer line but the $\Delta p/p$ of the actual beam may be uncertain when RF manipulations are done to modify bunch lengths before extraction. The rms betatron beam size is given by:

$$w_i = \sqrt{w_{i,\mathrm{meas.}}^2 - \left(D_i\,\Delta p/p\right)^2}$$

and, using Hereward's parameters $B(s)=\alpha(s)/\beta(s)$ and $G(s)=1/\beta(s)$, one can obtain the size and the shape of the

emittance ellipse at the first detector with the following expressions [6]:

$$\varepsilon = G_1 w_1^2 \ ,$$

with

$$G_1 = \frac{1}{m_{12} w_1} \sqrt{w_3^2 - w_1^2 \left(m_{11} - m_{12} B_1 \right)^2} \ .$$

and

$$B_1 = \frac{n_{12}^2 \left(m_{11}^2 - w_2^2 / w_1^2 \right) - m_{12}^2 \left(n_{11}^2 - w_3^2 / w_1^2 \right)}{2 m_{12} n_{12} \left(m_{11} n_{12} - n_{11} m_{12} \right)} \ ,$$

where m_{ij} and n_{ij} are the matrix elements of the 2x2 matrices M and N from the first to the second detector and from the first to the third detector, respectively.

Beamscope

In this method [7] applicable to circular machines, the beam is sent progressively onto a limiting aperture scraper, by means of a local bump. The remaining beam intensity is monitored with a BCT in terms of the bump distance to the scraper and the betatron amplitude distribution is deduced. The beam emittance can be computed from its rms value σ_a (see Table 1), knowing the beta value at the scraper position. The method, being destructive for the beam, is best suited to rapid cycling machines.

Screens

Since the development of CCD cameras and digital frame grabbers, screens are becoming interesting instruments for the measurement of precise beam profiles, and are therefore considered as alternatives to the more expensive SEM-Grids [8]. Screens have always to be considered together with their detector, CCD or tube camera. They have many advantages over grids.

First, the have finer resolution. A typical TV detector has a resolution of 288 x 384 pixels. This resolution is more or less degraded by the processing electronics and the transmission over copper or fibre optics cables which is characterised by the Modulation Transfer Function of the system [9]. Even for the worst cases, this resolution is far better than that of SEM-Grids, with typical pitch of 0.5 mm and 32 wires. The geometric reference for the monitor should always be given unambiguously by a reference pattern on the screen.

Second, there is no electric connection through the vacuum barrier and the resolution and covered aperture is a compromise which can be adjusted for each monitor by the optical set-up, and can be changed at will without breaking the vacuum, with standard screens covering the whole beam aperture.

Third, there is only one processing channel for all the information. Together with the excellent uniformity of modern CCDs, this is a definite advantage.

The only disadvantage of the screens was the material thickness of the usual luminescent screens [10], which resulted in non negligible beam blow-up of low energy beams, as compared to SEM-Grids. This is now disappearing with OTR (Optical Transition Radiation) screens, which can be used easily for beams with gamma above 20, which means for practically all lepton accelerators, including small Linacs, and proton beams above 20 GeV.

Luminescent screens being well known and described abundantly in the literature, only the OTR screens will be discussed further. Until recent work on OTR [11], they suffered from the suspicion of being severely limited in resolution by diffraction, diffraction increasing rapidly for high gamma beams. This is connected with the pecu-li–arities of the angular distribution of OTR, having an intensity hole in the direction of the light cone and a maximum at an angle $1/\gamma$, but fortunately long tails. OTR screens, depending only on the change of the dielec–tric constant at the vacuum/screen surface interface, can be very thin. Aluminium coated Mylar and titanium screens of the order of 10 μm thickness have been used. They are therefore not more beam disturbing than SEM Grids.

For proton beams of energy around 20 GeV as encountered in the SPS injection, the main limitation comes from the low light intensity and large central hole. Nevertheless, beam profiles were measured on three screens in the transfer channel from PS to SPS and compared to SEM Grid measurements. They gave similar results, with the added advantage of a larger number of points. Profiles were also measured on successive revolutions, up to 200, in the SPS to assess the perfect matching of a small LHC-type beam [12].

For leptons, profiles are measured in the SPS transfer lines with OTR screens on 3.5 GeV injected and 22 GeV ejected beams, corresponding to a maximum γ of 43,000. Variations of beam size as a function of observation wavelength give small variations in measured beam size, indicating that the diffraction limitation is not as severe as initially expected. Profiles with $\sigma \approx 1.4$ mm have been measured, and compare well with SEM-grid measurements, the difference being around 10%.

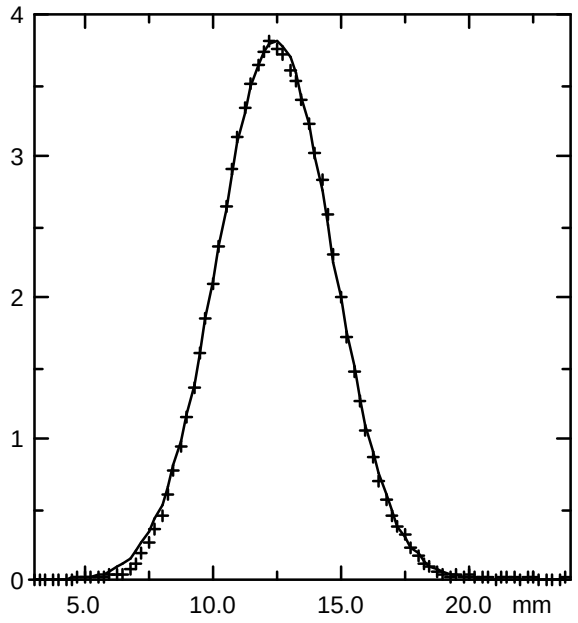

Fig. 4: Profile of a 22 GeV proton beam measured with a 12 μm OTR screen in the PS-SPS Transfer line TT10.

Wire scanners

Wire scanners are used in a wide range of accelerators to measure transverse beam profiles. They are not destructive for the beam and hence very useful in circular machines [13] [14] as well as in lepton linacs[15]. Charge depletion of the wire, forward scattered secondaries or gamma production by Bremsstrahlung in lepton machines, are the most commonly used signals. Wire scanners provide absolute measurements of the beam dimensions with an accuracy given by their mechanical design and by the reliability of the beam position measurement during the sampling time.

Some harmful effects are experienced by both the beam and the wire which can be minimised by an optimal choice of wire size, material and speed:

- Excessive heating may result in wire breakage. A first source of energy deposition inside the wire is by ionisation of the material's atoms. An efficiency between 30% and 50% has been quoted for this process [16] [17]. In lepton colliders the short bunches may in addition generate strong wake-fields which result in microwave heating of the wire. These electromagnetic interactions can be minimised by a smooth design of the monitor cross section and by choosing a wire made of an insulating material. In LEP, the choice of quartz wires instead of carbon allowed the raising of the maximum intensity from 2 mA to 8 mA [17].
- In circular machines, according to beam size and energy, the particles undergo Coulomb scattering inside the wire which can distort the measured profiles. This effect can be spotted, for instance, by comparing profiles measured in the two opposite directions (wire in/out)[18].
- In a cryogenics environment, one must also make sure that the flux of secondaries produced from the beam-wire interaction remains below the quench level of super conducting elements [19].

In order to get a good profile, the beam position must be stable during the whole sampling and the wire displacement between consecutive acquisitions must be smaller than one sigma of the measured profile. At CERN, wire speeds between 0.1 m/s and 20 m/s are used to scan with wires of diameters between 7 μm and 50 μm.

The ultimate resolution with a wire-scanner has been achieved in the FFTB at SLAC with a carbon wire of 4 μm. After quadratic de-convolution of the wire thickness, beam rms values of less than 1 μm could be determined [20].

Use of synchrotron light

Imaging Synchrotron Radiation (SR) Monitors give a transverse image of the beam, from which emittances can be calculated. A detailed description of the SR characteristics can be found in [21].

The main difference between protons and leptons is in the value of γ, the relativistic energy factor of the particle. As a consequence, the critical wavelength defining the 50% partition point of the radiated power, given by the formula:

$$\lambda_c = \frac{4\pi}{3}\frac{\rho}{\gamma^3}$$

with ρ the trajectory bending radius, is very different for the two types of beam. Whereas for leptons λ_C is already in the visible for the smallest accelerators, it is in the infrared for the highest energy proton accelerators. The SR energy decreases faster than exponentially as a function of wavelength below λ_C. There is then plenty of energy available to the usual imaging detectors, like CCD chips, in lepton machines, but far less, sometimes not enough, from proton beams. For proton machines it is then often necessary to use enhancement effects like the edge effect in bending magnets or special magnetic set-ups like undulators or wigglers [22].

The synchrotron light is emitted in a cone around the tangent to the trajectory. The horizontal band generated by the particles along their trajectory is cut out by the extraction mirror. Vertically, the apertures are in general large enough to contain most of the radiated power, and the natural opening angle defines the beam along this direction. For wavelengths much larger than λ_C, the natural opening angle of the SR is defined by:

$$\psi_{rms} \approx k\left(\frac{\lambda}{\rho}\right)^{1/3}$$

independent of beam energy. This is not the case for proton machines. These two limitations of the SR beam generate diffraction patterns which are a function of the

light wavelength. To decrease their contribution, the smallest possible wavelength is selected, at the limit of the visible and the UV for normal CCDs, i.e. 450 nm, or in the near UV for back illuminated CCDs and S20Q photo cathodes of Micro Channel Plate (MCP) intensifiers or TV tubes.

Finally, the position and the extent of the accepted light source is important for the precision of the beam profile measurement. Whereas this is not an important problem for small machines and for proton accelerators up to the highest energies achieved so far, because the useful light production is restricted to a small length, this is an important issue for larger lepton accelerators and for LHC in the TeV region. With a curvature radius of 3100 m, in LEP and LHC, this becomes a serious problem. In both machines, the light origin and acceptance has to be defined precisely, which is done with a slit, controlled in position and width, located at the focal point of the optical system.

These contributions to the measured profiles have to be subtracted to obtain the beam profile. If the Gaussian approximation is valid, this de-convolution becomes simply a quadratic subtraction of standard deviations:

$$\sigma_b^2 = \sigma_m^2 - \sigma_{Dy}^2 - \sigma_{LA}^2 - \sigma_i^2$$

where σ_b refers to the beam, σ_m to the measured spot size, σ_{Dy} to the horizontal or vertical diffraction, σ_{LA} to the longitudinal acceptance contribution and σ_i to an instrumental broadening, important when using a MCP.

The highest absolute precision is achieved by evaluating the various contributions to the beam profile broadening [23]. Cross-checks with reference monitors like Wire Scanners are performed to check the validity of the assumptions. For the UV telescopes of LEP (BEUV), the various contributions are:
σ_{DH}=320 μm, σ_{Dv}=230 μm, σ_{LA}=80 μm, σ_i= 110 μm.

In LEP, profile changes down to a few microns have been detected and an absolute emittance precision of 0.1 nm has been achieved at 45 GeV (see section 3).

Depending on the detector and its read-out electronics, either individual turns or the integral over several turns are acquired.

At high energy and/or high beam current in lepton machines, the deformation of the extraction mirror is another issue. This phenomenon became important at LEP above 87 GeV and 2 mA. The extraction Beryllium mirror deforms in a cylindrical way with a bending radius of the order of 500m at 91.5 GeV for a beam current of 2 mA. The defect can be corrected by changing the position of the detector to the image point for each plane. For larger deformations, expected when the beam energy will rise, adaptive optics comprising a deformable mirror and a variable position detector are considered, the optimum tuning being verified with so-called focus-scans.

Another alternative, to overcome the difficulties of extraction mirrors, is to make use of direct X-rays. This solution is adopted in LEP for the BEXE monitors where synchrotron radiation exits the machine vacuum chamber through a beryllium window 0.4 mm thick. The vertical distribution of X-rays is measured with an array of CdTe photo conductors mounted on a ceramic support. These detectors with 64 channels at a pitch of 100 μm are installed in an evacuated vessel with Kapton flat cables and can stand tremendous doses of radiation like 10^{15} Rad per year. They have been used to observe individual bunches of both beams for 1600 turns and revealed beam-beam quadrupolar oscillations [24]. With the advent of higher beam energies in LEP, the SR source has been displaced to a low field dipole and the distance of 100 m between the source and the detector allowed the introduction of an optional slit pinhole mid-way, which can be used to measure the beam size at the source [25].

Monitors using the ionisation of residual gas

In many machines, profile monitors are making use of the ionisation produced by the beam in the residual gas [26],[27],[28],[29]. Electrons/ions are drifted in an electric field of typically 400 V/cm and are collected on the strips of a cathode/anode to reconstruct the beam profile. At DESY [30] a SIT is used to produce a live TV image. In most cases the collected e^- or converted ions, are amplified through a MCP to gain a factor 10 to 10^4 in sensitivity. As it can be seen in Table 2, the pressure of the residual gas is very different from one machine to another and the integration times vary accordingly.

The beam space charge perturbs the linearity of the collecting field and must be corrected for, by the quantity:

$$\sigma_{cor.}^2 = \frac{\alpha I U r_p d}{e N c} \sqrt{\frac{2 m_p}{e V}} \frac{\sigma_x}{\sigma_y},$$

where α is a fit parameter, I: beam current, U: accelerator circumference, r_p: classical proton radius, d: space between the collecting grids, e: elementary charge, N: number of bunches, c: velocity of light, m_p: proton mass (for H_2 ions), V: voltage between the grids.

Other effects contribute to the image broadening and can also be subtracted in quadrature like the ions transverse energy: σ_i = 290 μm and the camera definition: σ_t = 70 to 200 μm. The real beam size then reads:

$$\sigma_{beam}^2 = \sigma_{meas.}^2 - \sigma_{cor.}^2 - \sigma_i^2 - \sigma_t^2 .$$

Table 2. Some technical specifications of residual gas ionisation beam profile monitors

Laboratory/machine	Particle type	E_{min}	E_{max}	P_{gas} [Pa]	I_{beam}	σ_{min} [mm]	σ_{max} [mm]	$\sigma_{cor.}$ [mm]	Integration time
HERAp	p	40 GeV	820 GeV	10^{-7}	5–200 mA	1	2	1	40 ms
GANIL (transfer line)	ions		100 MeV	10^{-5}	1 nA–2.2µA	.4	1.3	.2	10 ms–5 s
FNAL booster	p	0.4 GeV	8 GeV	7×10^{-7}	21 µA	2	7	•3	1.6 µs
CRYRING	D^+	12 MeV	16 MeV	2×10^{-10}	10 µA	.34	3	0	1 min

CCD based detectors

The CCD is an extremely powerful detector for the measurement of beams [9]. As it is a component used in commercial TV cameras, the whole range, including the so-called scientific grade components, benefit from the large R&D investment in the field. Radiation harder CID chips exist for the nuclear industry. They are working on the individual pixel matrix readout principle, different from the pixel serial readout of normal CCDs. They will not be dealt with further here, as for a CCIR TV readout they are identical to CCDs and can use the same Frame Grabbers. Nevertheless, they cannot be used for the special modes described in Ref. [9].

The dynamic range of the CCDs are in excess of 12 bits, and the uniformity of the detector sensitivity is of the same order for high quality types. The spectral sensitivity goes from 450 to 1200 nm. The limit has been extended towards the UV either by depositing on the surface a scintillator sensitive to UV and re-emitting in the bandwidth of the normal CCD, or by illuminating from the backside a thinned CCD. The cost of the first type of UV sensitive CCD is far below the second type, but its performance, in sensitivity and resolution, is also much lower.

3 COMPARATIVE MEASUREMENTS

CERN injectors

In view of delivering a bright beam for filling the LHC, a series of measurements were done in the injector chain between 50 MeV and 26 GeV. The results are commented upon in Refs. [31] and [32] from which the summary picture shown in Fig. 5. is taken.

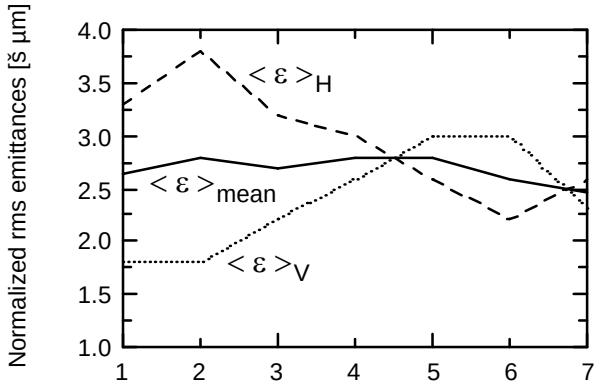

Fig. 5. Normalised rms emittances measured in the chain of LHC injectors (1.4 GeV to 26 GeV):
1: CPB (PS booster) at 1.4 GeV, Beamscope
2: CPB measuring line at 1.4 GeV, SEM grids
3: PS injection line at 1.4 GeV, SEM grids
4: PS at 1,4 GeV, wire scanner
5: PS at 10 GeV, wire scanner
6: PS at 26 GeV, wire scanner
7: TT2 transfer line from PS, SEM wires (0.35 mm)

The first two measurements are not accurate enough for the small LHC beam emittances of 3 µm, but the high resolution SEM wires used in TT2 give reliable results [33]. The successful test of a prototype fast wire scanner in the PSB [34] shows that more accurate measurements will be available with the implementation of these new monitors. Finally a new injection matching technique is also being tested in the CPS, following the ideas of Ref. [12].

LEP

The evaluation of beam emittances from beam size measurements taken at different monitor locations necessitates a precise knowledge of the beam optics functions at these monitors which in large machines is a source of uncertainty due to β-beating.

In LEP, a cross calibration was made between Wire Scanners and synchrotron light monitors (BEUV) used in operation in 1995 and gave excellent results at 68 GeV. The optics functions were measured at the different monitors with harmonic analysis of betatron oscillations [35] and the relative effect of the blow-up, of the order of 15% on the smallest distribution width measured with

Wire Scanners, was subtracted. An agreement of better than 0.1 nm was then obtained between the two monitors down to a vertical emittance of 0.2 nm (see Fig. 6).

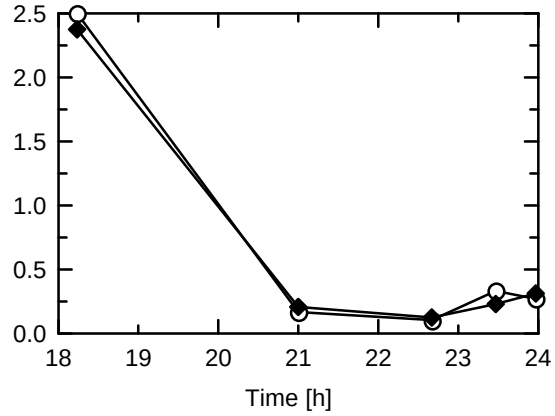

Fig. 6. Cross calibration of emittance monitors at LEP: white circles: BEUV, black diamonds: Wire Scanner.

Since LEP has reached energies beyond 80 GeV the beryllium mirrors used to extract the SR light for the BEUV telescopes, are being deformed by the deposited heat and cannot anymore be used for very accurate measurements. The X-ray BEXE detectors still can be trusted for accurate measurements of the photon vertical emittance. But in order to relate it to the lepton beam emittance, the lattice functions have also to be precisely known. A dedicated cross-calibration was done on the 23.10.97 between BEXE and Wire Scanner detectors and gave 180±20 pm and 280±20 pm for e^+ and e^- beams respectively, which are remarkably close results.

The problem of determining emittances at LEP is now mainly related to the knowledge of lattice functions, which are changing drastically, according to modifications in the RF cavity distribution [36]. Even smaller beam emittances have been measured in LEP with BEXE using the slit-pinhole technique [25] which will be further improved for 1998 with a vertical mechanical adjustment of the slit. For very small emittances, Wire Scanners should be used with 10 μm diameter quartz wires and a reduced speed of 0.1 m/s.

REFERENCES

[1] F.J. Sacherer, IEEE Trans. Nucl. Sci. NS-18 (1971) pp. 1105-8.

[2] Y. Yamazaki et al., Nucl. Instrum. Methods Phys. Res., A : 322 (1992) pp. 139-145.

[3] U. Raich and J.M. Nonglaton, Proc. ICALEPCS, Berlin, October 18-22, 1993, pp.

[4] M.C. Ross et al., PAC'1987, Washington, Proc. IEEE 87CH2387-9, pp. 725-728.

[5] C. Metzger, CERN/SI/Int. DL/69-10, 24 October, 1969.

[6] P. Brummer, CERN-ISR-OP 72-6, 26 January, 1972.

[7] H. Schönauer, IEEE Trans. Nucl. Sci., Vol. NS-26, 1979, pp. 3294, and Proc. Work. Adv. Beam Instrum., Tsukuba, April 22-24, 1991, Vol. 2, pp.453-466.

[8] J. Camas et al., Proc. DIPAC'95, pp. 57-60.

[9] R.J. Colchester et al., BIW, Argonne, May, 1996, AIP Conf. Proc. 390, pp. 215-222.

[10] J. Camas et al., PAC'93, pp. 2498-2500.

[11] R.B. Fiorito and D.W. Rule, BIW, Santa Fe, October, 1993, AIP Conf. Proc. 319, pp. 21-37.

[12] C. Bovet and R. Jung, LHC Project Report 3, Rev., and Proc. EPAC'96, pp. 1597-9.

[13] A. Barisy et al., Proceedings IEEE Trans. Nucl. Sci. : 28 (1981) pp. 2180-2182.

[14] Ch. Steinbach and M. van Rooij, PAC'85, IEEE Trans. Nucl. Sci, Vol. NS-32, 1985, pp. 1920-2.

[15] M.C. Ross et al., Proc. PAC'91, San Francisco, May 6-9, 1991, pp. 1201-1203.

[16] J. Bosser et al., CERN SPS/86-26 (MS).

[17] C. Fischer et al., BIW, Argonne, May, 1996, AIP Conf. Proc. 390, pp. 290-297.

[18] J. Camas et al., PAC'93, pp. 2504-7.

[19] J. Bosser and C. Bovet, LHC Project Note 108, September, 1997.

[20] C. Field, Nucl. Instrum. Methods Phys. Res., A: 360 (1995) pp. 476-475.

[21] A. Hofmann, CERN LEP-DI/89-55.

[22] R. Bossart et al., Nucl. Instrum. Methods Phys. Res., A: 164 (1979) pp. 375-380.

[23] Castro et al., SL MD Note 202, February, 1996.

[24] C. Bovet et al., DIPAC'95, Travemünde, 28-31 May, 1995, DESY M-9507, pp. 102-105.

[25] C. Bovet et al. in these Proceedings.

[26] T. Kawakubo et al., Particle Accelerators, 1990, Vol. 29, pp. 233-238.

[27] R. Anne et al., Nucl. Instrum. Methods Phys. Res., A: 329 (1993) pp. 21-28.

[28] T. Quinteros et al., Nucl. Instrum. Methods Phys. Res., A: 333 (1993) pp. 288-293, and ibid, A: 378 (1996) pp. 35-39.

[29] W. S. Graves et al., Nucl. Instrum. Methods Phys. Res., A: 364 (1995) pp. 13-18.

[30] K. Wittenburg, Proc. Int. Workshop Part. Dyn. Acc., 21-26 November, 1994, Tsukuba, pp. 72-84.

[31] R. Cappi, Proc. Int. Workshop Part. Dyn. in Acc., 21-26 November, 1994, Tsukuba, pp. 12-27.

[32] K. Schindl, to be published in Particle Accelerators

[33] H. Koziol, Private Communication.

[34] M. Arruat et al., in these Proceedings.

[35] P. Castro, CERN SL/96-70 (BI), 25 Nov., 1996.

[36] J. M. Jowett, SL MD Note 240, revised and corrected on 27 Aug., 1997.